*Electronic Supplementary Information*

# Mechanochromic aromatic hydrocarbons that bear one simple substituent

Tomohiro Seki*[a] and Kota Hattori[a]

Department of Chemistry, Faculty of Science, Shizuoka University, Shizuoka City, Shizuoka 422-8529, Japan

Email: seki.tomohiro@shizuoka.ac.jp

## Contents

## 1. General

All commercially available reagents and solvents are of reagent grade and were used without further purification unless otherwise noted. Solvents for the synthesis were purchased from commercial suppliers, degassed by three freeze-pump-thaw cycles and further dried over molecular sieves (4 Å). Purification by column chromatography was performed with a silica gel 60N (spherical, neutral, 40–100 μm mesh, Kanto chemicals, Japan). NMR spectra were recorded on a JEOL ECA-600 spectrometer ($^{1}$H: 600 MHz; $^{13}$C: 151 MHz) using tetramethylsilane and $CDCl_3$ as internal standards, respectively. UV-vis absorption spectra were recorded on a JASCO V-750 spectrometer. The absorption spectra of the solid samples were recorded on a JASCO V-750 spectrophotometer equipped with JASCO ISV-922 integrating sphere. Emission and excitation spectra were recorded on a JASCO FP-8600 spectrometer. Luminescence microscopic spectra were recorded on a Photonic Hamamatsu PMA-12 Multichannel Analyzer (C14631-01). A cooling/heating stage on JHC 10002L was used for temperature changes of solid samples. The emission quantum yields of the solid samples were recorded on a JASCO ILF-835 integrating sphere that was interfaced with a JASCO, FP-8600 spectrofluorometer. Emission lifetime measurements were recorded on a Hamamatsu Quantaurus-Tau spectrometer. High resolution mass spectra were recorded on a Thermo Scientific Exactive at the Center for analytical instrumentation at Chiba University. Photographs were obtained using Olympus BX53 or SZX10 microscopes with Olympus DP74, Sony α7S digital cameras. Differential scanning calorimetry (DSC) measurements were recorded on a Shimadzu DSC60 instrument using $Al_2O_3$ as a reference material. Powder diffraction data were recorded at on a Rigaku SmartLab diffractometer with Cu-$K_\alpha$ radiation with a monochrometer. TGA traces were recorded on a Rigaku TG 8121.

***Single crystal X-ray diffraction analyses***: A suitable crystal was mounted with Paratone oil on a MiTeGen MicroMounts and transferred to the Four-circle Kappa Geometry Goniometer of a RIGAKU XtaLAB Synergy-S system with 1.2 kW PhotonJet-S microfocus rotating anode using graphite monochromated Cu-$K_a$ radiation and HyPix-6000HE detector. Cell parameters were determined and refined, and raw frame data were integrated using CrysAlis$^{Pro}$ (Agilent Technologies). The structures were solved by direct methods with (SHELXT)[S1] and refined by full-matrix least-squares techniques against $F^2$ (SHELXL-2018/3)[S2] by using Olex2 software package.[S3] The intensities were corrected for Lorentz and polarization effects. The non-hydrogen atoms were refined anisotropically. Hydrogen atoms were placed using AFIX instructions. Simulated powder patterns were generated with Mercury software[S4] from the structures determined by single-crystal diffraction analyses.

## 2. Synthesis

*Synthesis of **4***

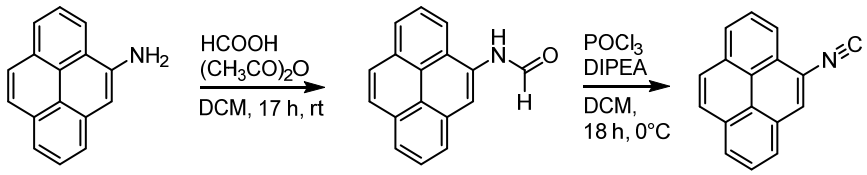


After an oven-dried screw neck reaction vial containing a magnetic stir bar was sealed with a screw cap containing a Teflon-coated rubber septum, it was connected to a vacuum/nitrogen manifold through a rubber tube. It was evacuated and then backfilled with nitrogen. This cycle was repeated three times. Then, formic acid (322 mg, 7.0 mmol, 2.0 equiv) and acetic anhydride (715 mg, 7.0 mmol, 2.0 equiv) were added. The mixture was stirred at 60°C for 2 h for *in-situ* preparation of acetic formic anhydride. A solution of 4-aminopyrene[S5] (761 mg, 3.5 mmol) in $CH_2Cl_2$ (35 mL) was prepared in another oven-dried two-neck round-bottom flask, and the preformed acetic formic anhydride solution was injected to the 4-aminopyrene solution at 0°C. After stirring the resulting solution at rt for 17 h, sat. aq. $NaHCO_3$ solution was added to quench the reaction. The resulting precipitate was obtained by filtration and washed with $H_2O$, MeOH and then $Et_2O$. The resulting solid was dried under reduced pressure which gave formamide as a white solid. This was used for the next step without further purification.

An oven-dried two-neck round-bottom flask was connected to a vacuum/nitrogen manifold through a rubber tube. It was evacuated and then backfilled with nitrogen. This cycle was repeated three times. This flask was charged with *N*-(pyrene-4-yl)formamide prepared by the above procedure. The $CH_2Cl_2$ (30 mL) and *N*-ethyldiisopropylamine (1.940 g, 15 mmol, 5.0 equiv) were added. $POCl_3$ (920 mg, 6.0 mmol, 2.0 equiv) was added dropwise at 0°C. After stirring at 0°C for 17 h, the reaction mixture was diluted with $CH_2Cl_2$, and washed with sat. aq. $NaHCO_3$ solution. The solution was extracted with $CH_2Cl_2$, and then washed with $H_2O$. The combined organic layers were dried over $Na_2SO_4$ and then evaporated in vacuo. The residue was purified by column chromatography on silica gel ($CH_2Cl_2$/hexane = 3:1) to give an analytically pure **4** as white solid (589 mg, 2.6 mmol, 86%).

$^1$H NMR (600 MHz, $CDCl_3$, δ): 8.04 (t, *J* = 7.8 Hz, 1H), 8.07 (d, *J* = 8.4 Hz, 1H), 8.09 (d, *J* = 9.0 Hz, 1H), 8.13 (t, *J* = 7.8 Hz, 1H), 8.17 (d, *J* = 7.2 Hz, 1H), 8.18 (s, 1H), 8.25 (d, *J* = 7.2 Hz, 1H), 8.27 (d, *J* = 7.8 Hz, 1H), 8.48 (d, *J* = 7.8 Hz, 1H). $^{13}$C NMR (151 MHz, $CDCl_3$, δ): 120.7 (*C*H), 123.0 (*C*NAr), 123.7 (*C*), 124.4 (*C*), 125.0 (*C*), 125.9 (*C*H), 126.1 (*C*H), 126.6 (3*C*H), 127.0 (*C*H), 127.50 (*C*H), 127.54 (*C*H), 129.0 (*C*), 130.9 (*C*), 131.1 (*C*), 167.2 (*C*). MS-ESI (*m*/*z*): $[M+H]^+$ calcd for $C_{17}H_{10}N$, 228.0808; found, 228.0806. Anal. Calcd for $C_{17}H_9N$: C, 89.84; H, 3.99; N, 6.16. Found: C, 89.78; H, 3.95; N, 6.09.

-

*Synthesis of **1***

Pyrene **1** was reported previously,[S6] and we also prepared **1** according to the procedure described for **4**. NMR spectra of **1** agreed well with that previously reported.

## 3. Photophysical properties of 1 and 4

**Table S1** Photophysical properties of **1** and **4**.

| | $\Phi_{em}$ / % [a] | $\tau_{av}$ / ns ($\lambda_{em}$ / nm)[a,b] | $\tau_1$ / ns ($A$ / -) | $\tau_2$ / ns ($A$ / -) |
|---|---|---|---|---|
| **1** | 48 | 61 (495) | 61 (1.00) | - |
| **1** in $CH_2Cl_2$[c] | 30 | 13 (383) | 13 (1.00) | - |
| **4** | 51 | 38 (452) | 29 (0.72) | 52 (0.28) |
| **4** in $CH_2Cl_2$[c] | 25 | 17 (379) | 17 (1.00) | - |

[a]: $\lambda_{ex}$ = 365 nm. [b]: $\tau_{av} = (\tau_1^2 A_1 + \tau_2^2 A_2 + \cdots) / (\tau_1 A_1 + \tau_2 A_2 + \cdots)$. [c] $c$ = 5.0 µM

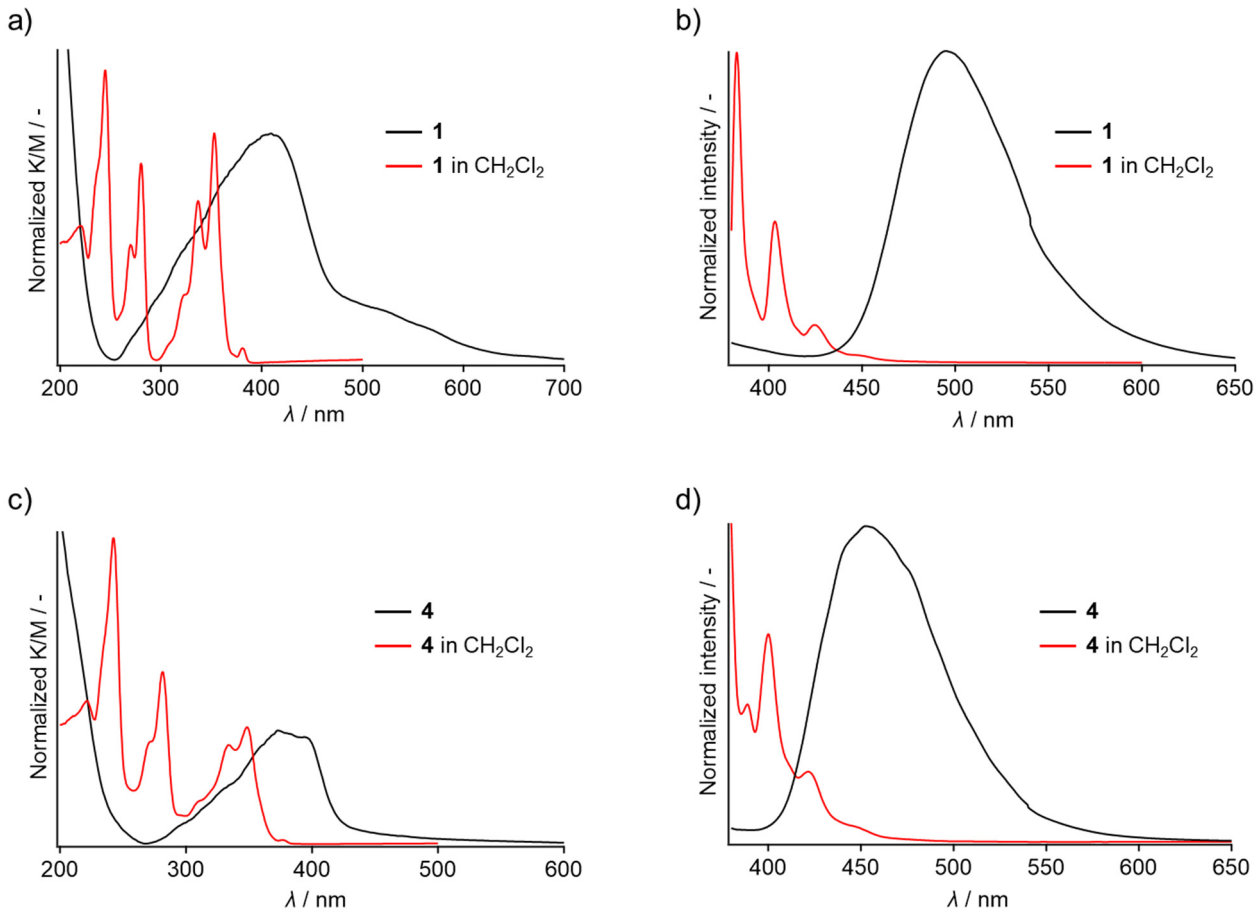


**Fig. S1** a,c) Absorption and b,d) emission spectra ($\lambda_{ex}$ = 365 nm) of a monomeric state (in $CH_2Cl_2$, $c$ = 5.0 µM, red lines) and solid state (black lines) of a,b) **1** and c,d) **4**).

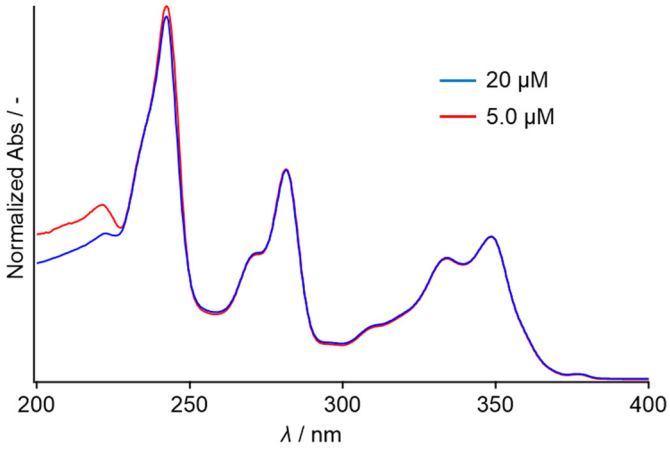


**Fig. S2** Concentration-dependent UV-vis absorption spectra of **4** in $CH_2Cl_2$ ($c$ = 5.0 or 20 μM). Spectral overlap indicates the monomeric nature of **4** under this concentration range although the absorption band is relatively broad.

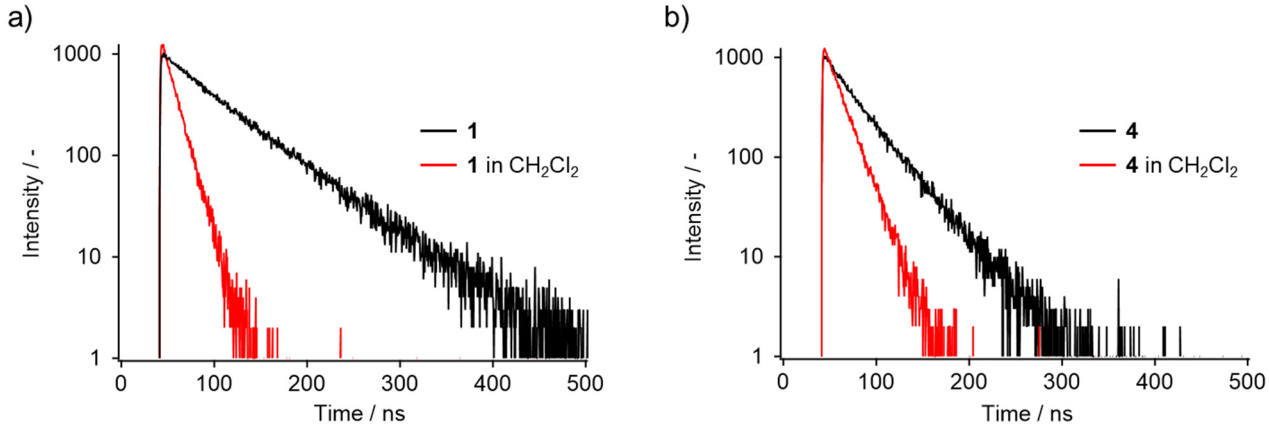


**Fig. S3** Emission decay profiles of a) **1** and b) **4** in solid and solution state (in $CH_2Cl_2$, $c$ = 5.0 μM). Excitation wavelength: 365 nm. Monitoring emission wavelengths are summarized in Table S1.

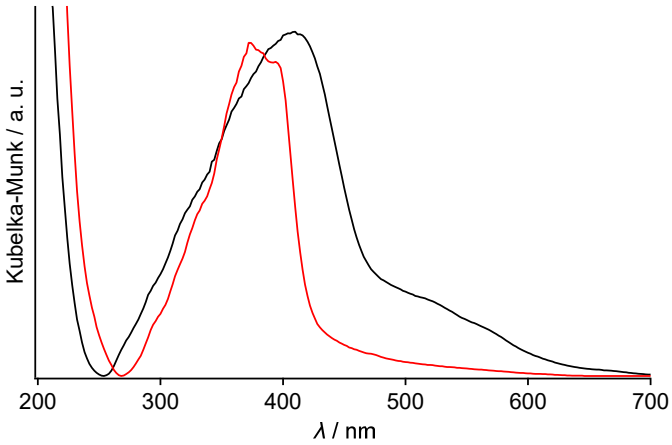


**Fig. S4** Normalized absorption spectra of the solid sample of **1** (black line) and **4** (red line) based on the diffuse reflection spectra.

## 4. Structure analyses of 1 and 4

**Table S2** Summary of X-ray crystallographic data

| crystal | **1**[e] | **4** |
|---|---|---|
| CCDC Number | - | 2312583 |
| Empirical Formula | $C_{17}H_9N$ | $C_{17}H_9N$ |
| Formula Weight | 227.25 | 227.25 |
| Crystal System | triclinic | monoclinic |
| Crystal Size / mm | 0.83×0.34×0.12 | 0.41×0.03×0.03 |
| *a* / Å | 6.8755(4) | 3.8023(2) |
| *b* / Å | 8.5851(4) | 17.9097(9) |
| *c* / Å | 9.9559(6) | 15.9061(8) |
| *α* / ° | 105.752(5) | 90 |
| *β* / ° | 97.935(5) | 93.960(4) |
| *γ* / ° | 98.993(5) | 90 |
| *V* / Å$^3$ | 548.48(6) | 1080.59(10) |
| Space Group | *P*-1 | $P2_1/c$ |
| *Z* value | 2 | 4 |
| $D_{calc}$ / g cm$^{-3}$ | 1.376 | 1.397 |
| Temperature / K | 100.00(10) | 100.00(10) |
| $2\theta_{max}$ / ° | 154.694 | 154.162 |
| $\mu$(Cu K$_\alpha$) / mm$^{-1}$ | 0.623 | 0.632 |
| No. of Reflections | 6239 | 5540 |
| $R_1$[a] | 0.0422 | 0.0870 |
| $wR_2$[b] | 0.1401 | 0.2583 |
| GOF[c] | 1.107 | 1.119 |
| Max./Mini. peak *I*[d] / Å$^3$ | 0.26/−0.23 | 0.91/−0.34 |

[a]: $I > 2.00\sigma(I)$. [b]: All reflections. [c]: Goodness of Fit Indicator. [d]: in Final Diff. Map. [e]: This crystal structure was reported previously.[S7]

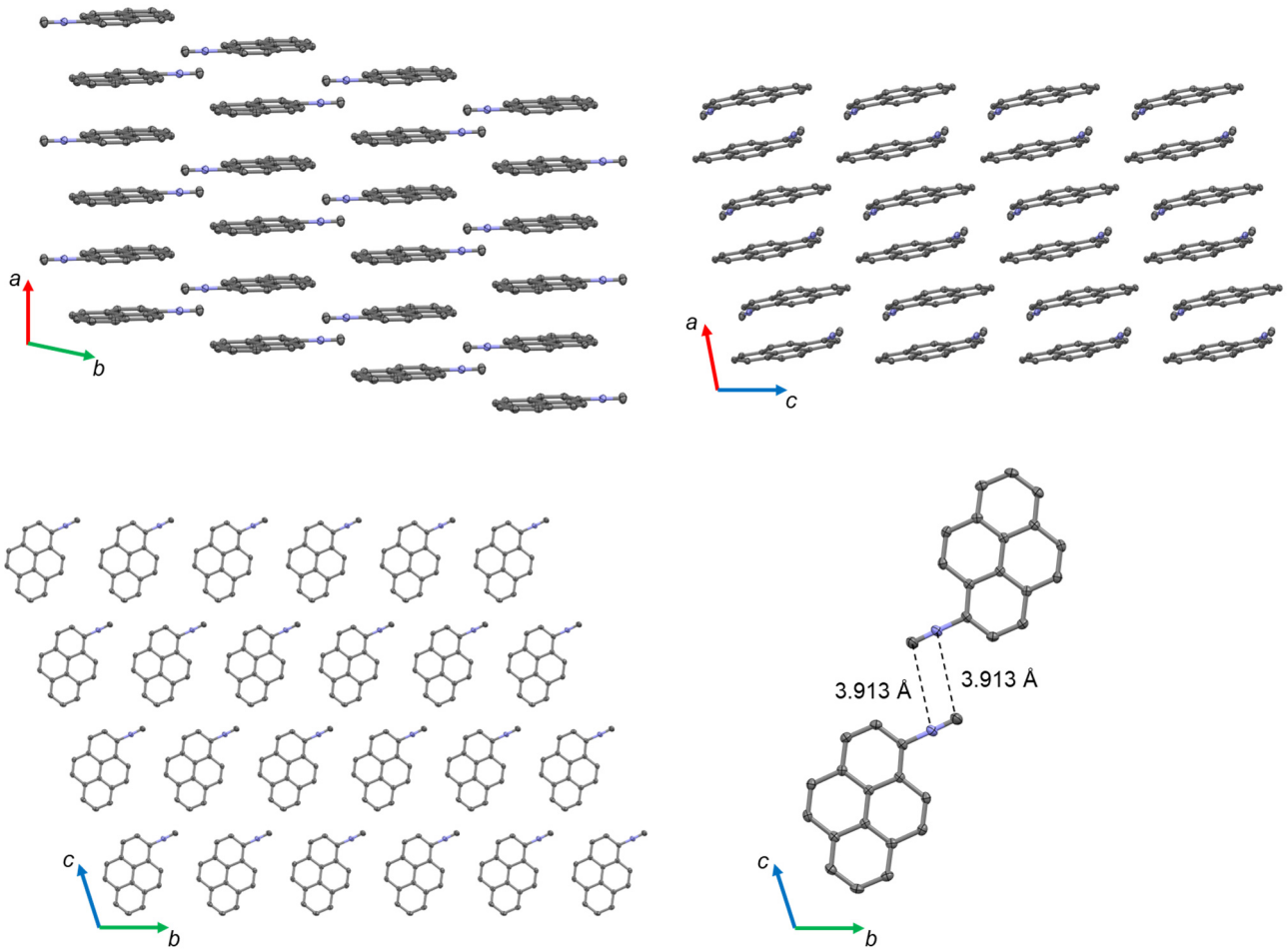


**Fig. S5** Single crystal structure of **1**.

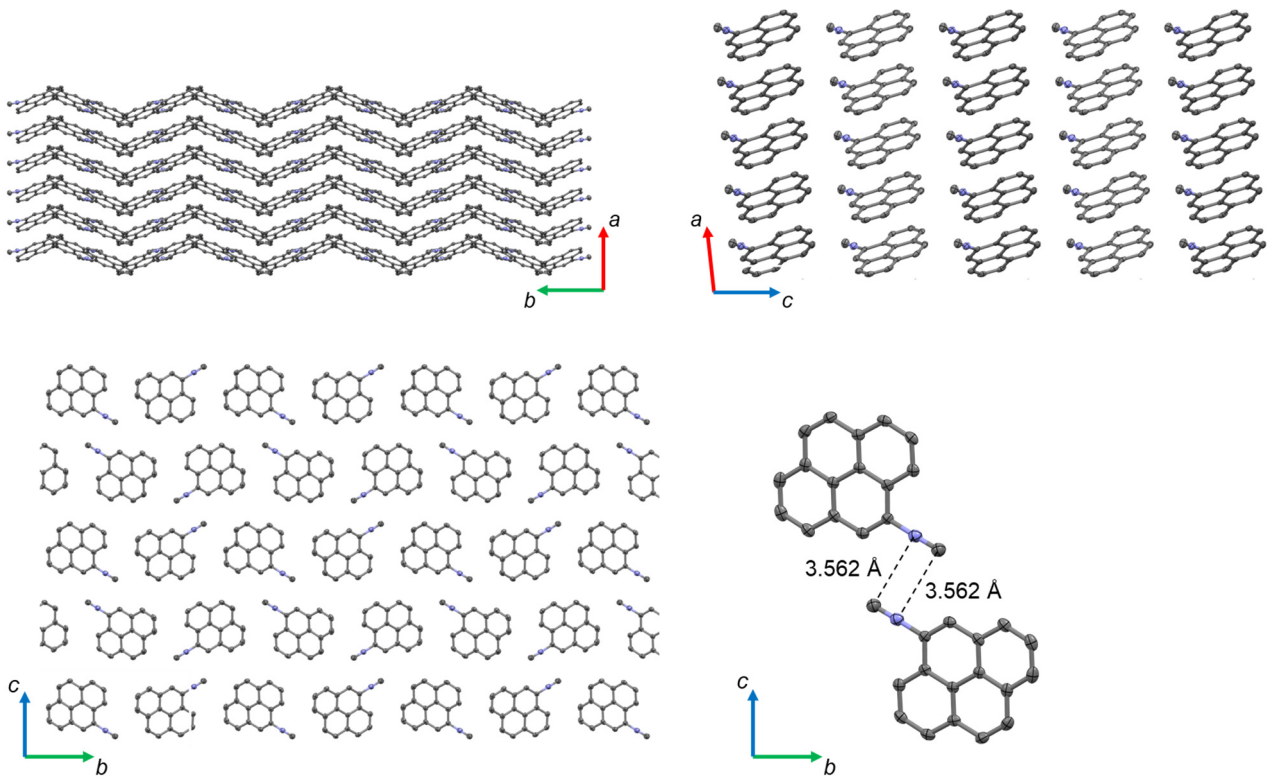


**Fig. S6** Single crystal structure of **4**.

## 5. Theoretical analyses of 1 and 4

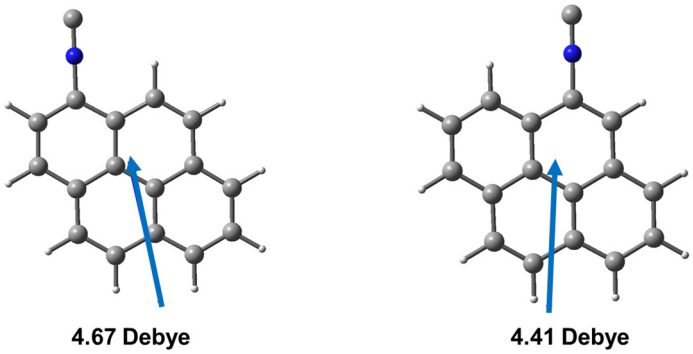


**Fig. S7** Optimized structure of a monomer under vacuum condition (b3lyp/6-31+g(d)).
All calculations were performed using the Gaussian 09W (revision C.01) and Gaussian 09 program packages.[S8] In the calculations, the 6-31+g(d) basis set and B3LYP functionals were used and estimated the dipole moment of **1** and **4**. Molecular orbitals were drawn using GaussView 6.1.1.

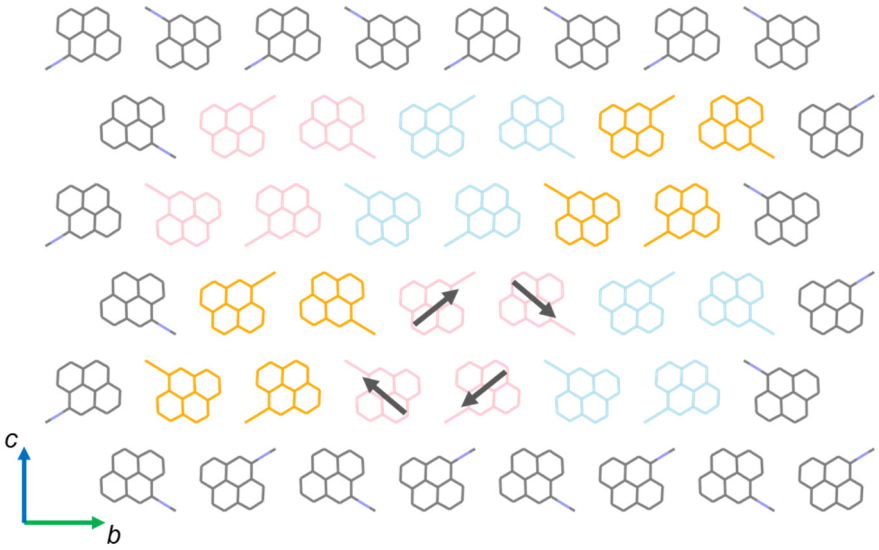


**Fig. S8** Schematic representation of the dipole moment (depicted by the arrows) within the *bc* plane of the crystalline lattice of **4**.

## 6. Photophysical properties of the ground phases

**Table S3** Photophysical properties of **1**, **1**$_{after}$, **4** and **4**$_{after}$.

| | $\Phi_{em}$ / % [a] | $\tau_{av}$ / ns ($\lambda_{em}$ / nm)[a,b] | $\tau_1$ / ns ($A$ / -) | $\tau_2$ / ns ($A$ / -) |
|---|---|---|---|---|
| **1** | 48 | 61 (495) | 61 (1.00) | - |
| **1**$_{after}$ | 37 | 45 (478) | 20 (0.32) | 50 (0.68) |
| **4** | 51 | 38 (452) | 29 (0.72) | 52 (0.28) |
| **4**$_{after}$ | 33 | 31 (470) | 16 (0.66) | 43 (0.34) |

[a]: $\lambda_{ex}$ = 365 nm. [b]: $\tau_{av} = (\tau_1^2 A_1 + \tau_2^2 A_2 + \cdots) / (\tau_1 A_1 + \tau_2 A_2 + \cdots)$.

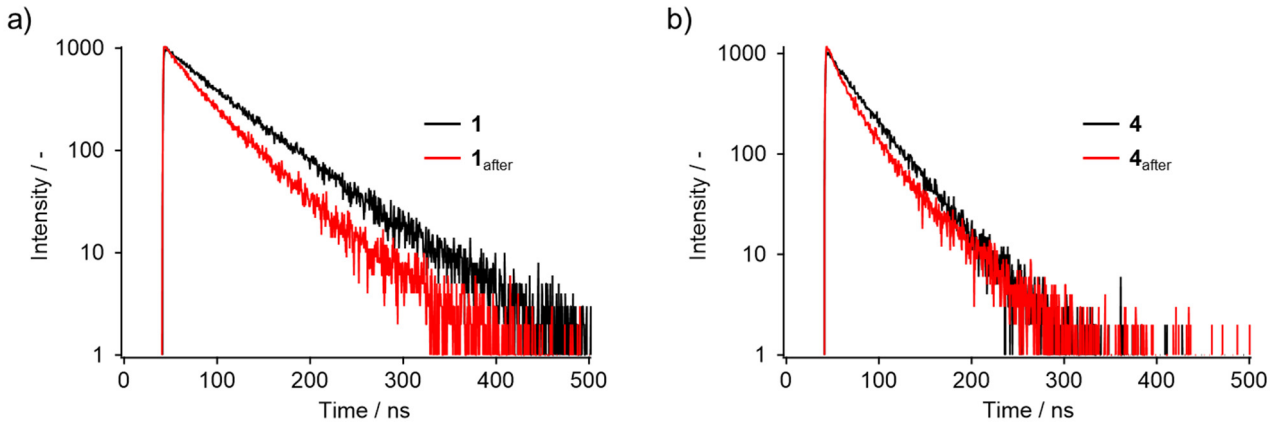


**Fig. S9** Emission decay profiles of a) **1** (monitored at 495 nm), **1**$_{after}$ (monitored at 478 nm), b) **4** (monitored at 452 nm) and **4**$_{after}$ (monitored at 470 nm). Excitation wavelength are 365 nm.

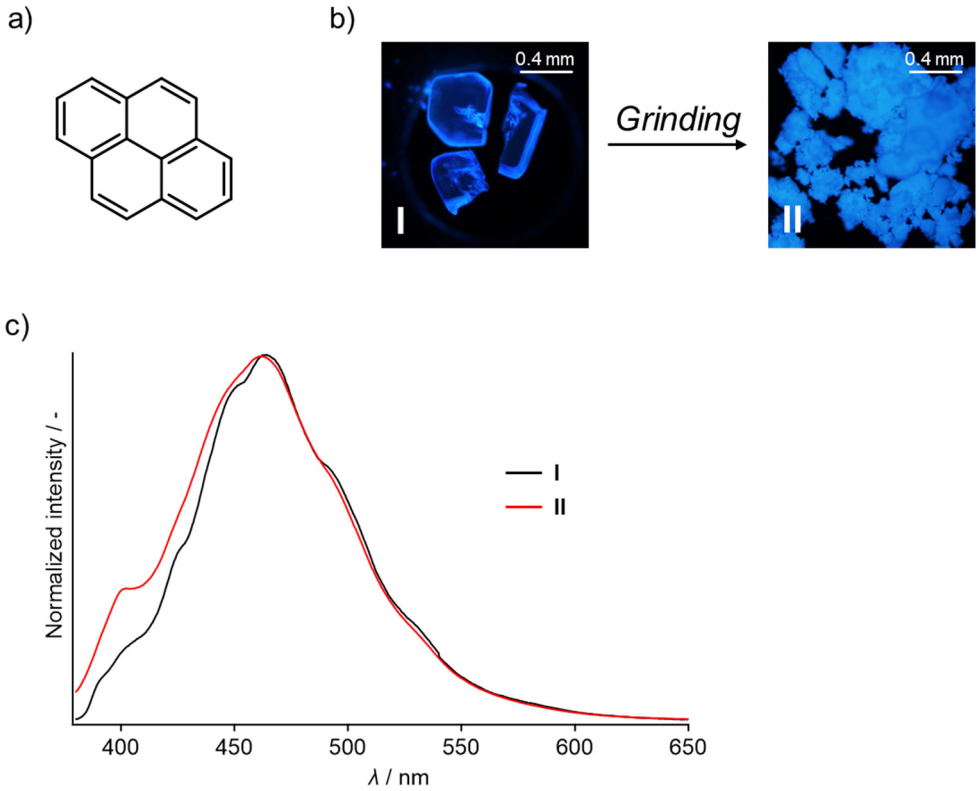


**Fig. S10** a) Chemical structure of unsubstituted pyrene. b) Photographs of pyrene before and after mechanical stimulation taken under UV light (365 nm). c) Emission spectra of solid sample of pyrene upon excitation at 365 nm.

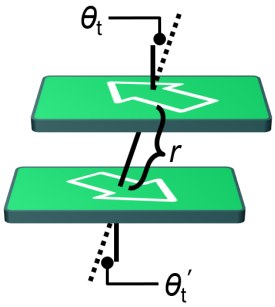


$\theta_r = 180°$

**Fig. S11** Schematic representation of torsional angle $\theta_t$ within the stacked dimer. As reported previously,[S9] dipole–dipole interactions are affected by $\theta_t$ and $\theta_r$ as well as dipole moment and relative distance ($r$).

## 7. Thermal Responses of 1 and 4

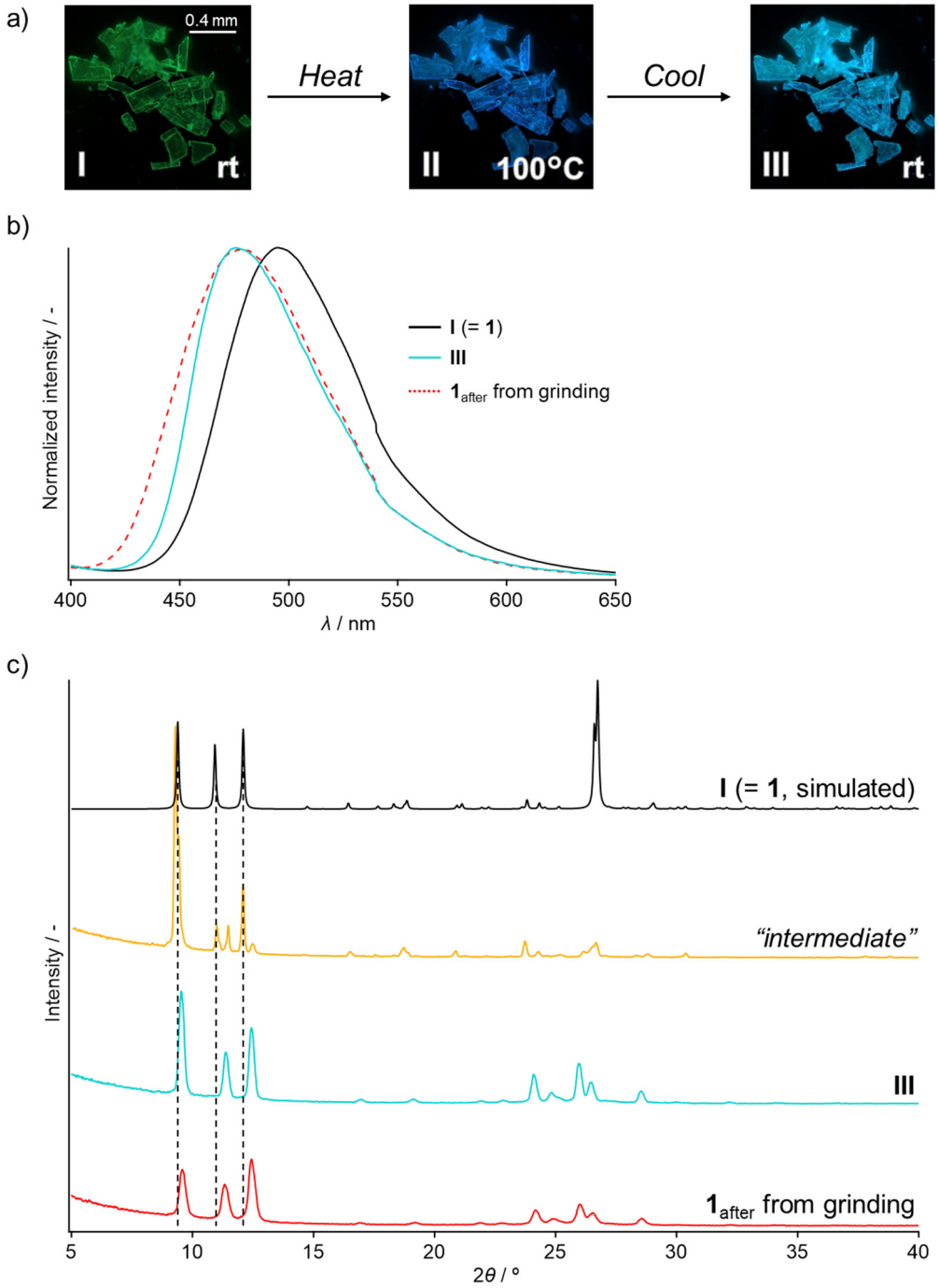


**Fig. S12** a) Photographs of **1** upon heating and subsequent cooling (under UV light). b) Emission spectra of **1** [the sample denoted as "**I**" in a), black line], the thermally treated sample [denoted as "**III**" in a), light blue line] and $\mathbf{1}_{after}$ obtained by grinding (reference, red dotted line). Excitation at 365 nm. c) A simulated powder pattern of **1** [the sample denoted as "**I**" in a), black line] and PXRD patterns of the thermally treated sample [denoted as "**III**" in a), light blue line] and $\mathbf{1}_{after}$ obtained by mechanical stimulation (red line; the reference sample). The yellow line in c) is the PXRD pattern of the "intermediate" sample of **1**, which was obtained from heating for a short time and then cool to rt This indicates the coexistence of the original **1** and $\mathbf{1}_{after}$.

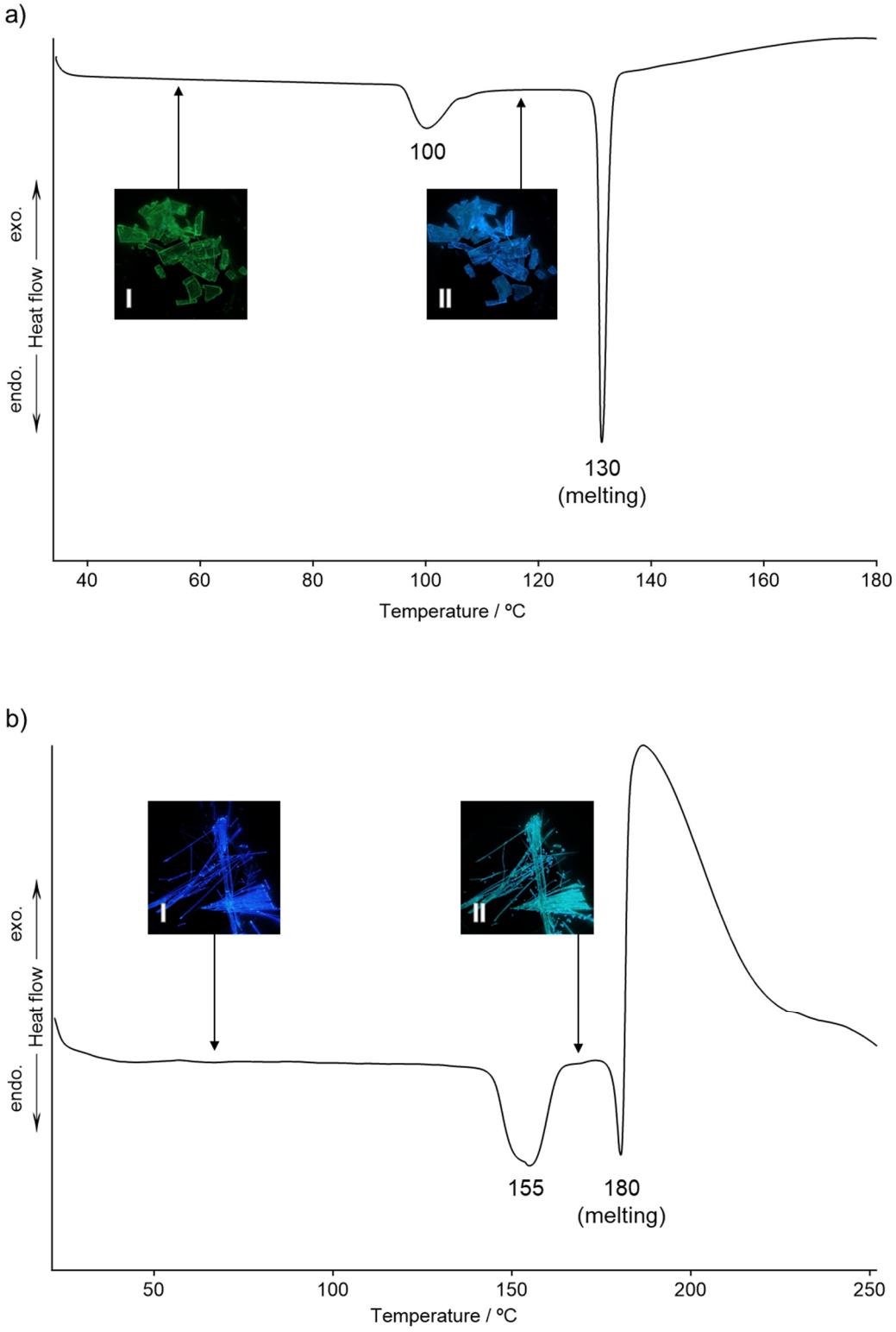


**Fig. S13** DSC traces of a) **1** and b) **4** with a heating rate of 5.0°C/min.

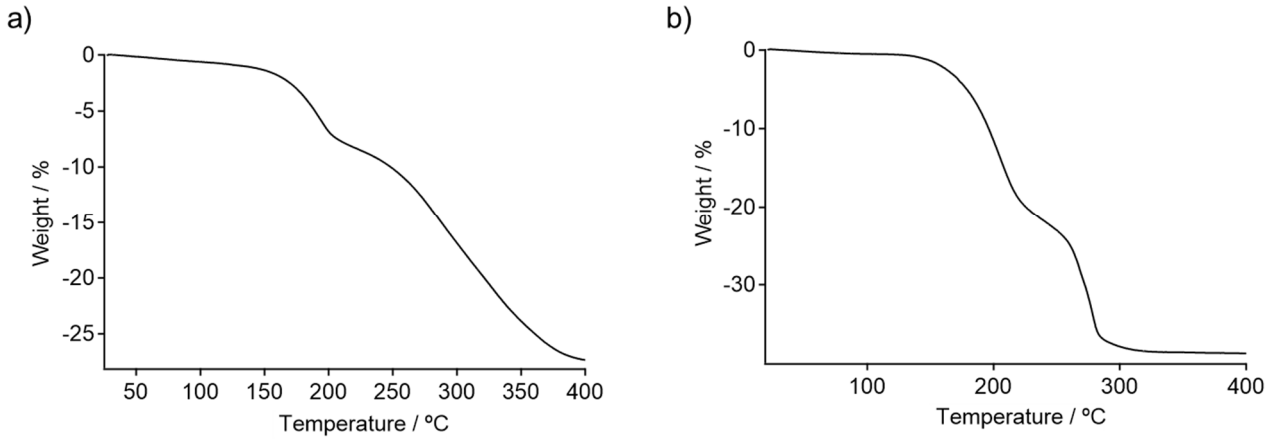


**Fig. S14** Thermogravimetric traces of a) **1** and b) **4** with a heating rate of 4.0°C/min.
Note: Below the phase transition temperature (100°C for **1** and 155°C for **4**), **1** and **4** did not show clear decrease of the weight.

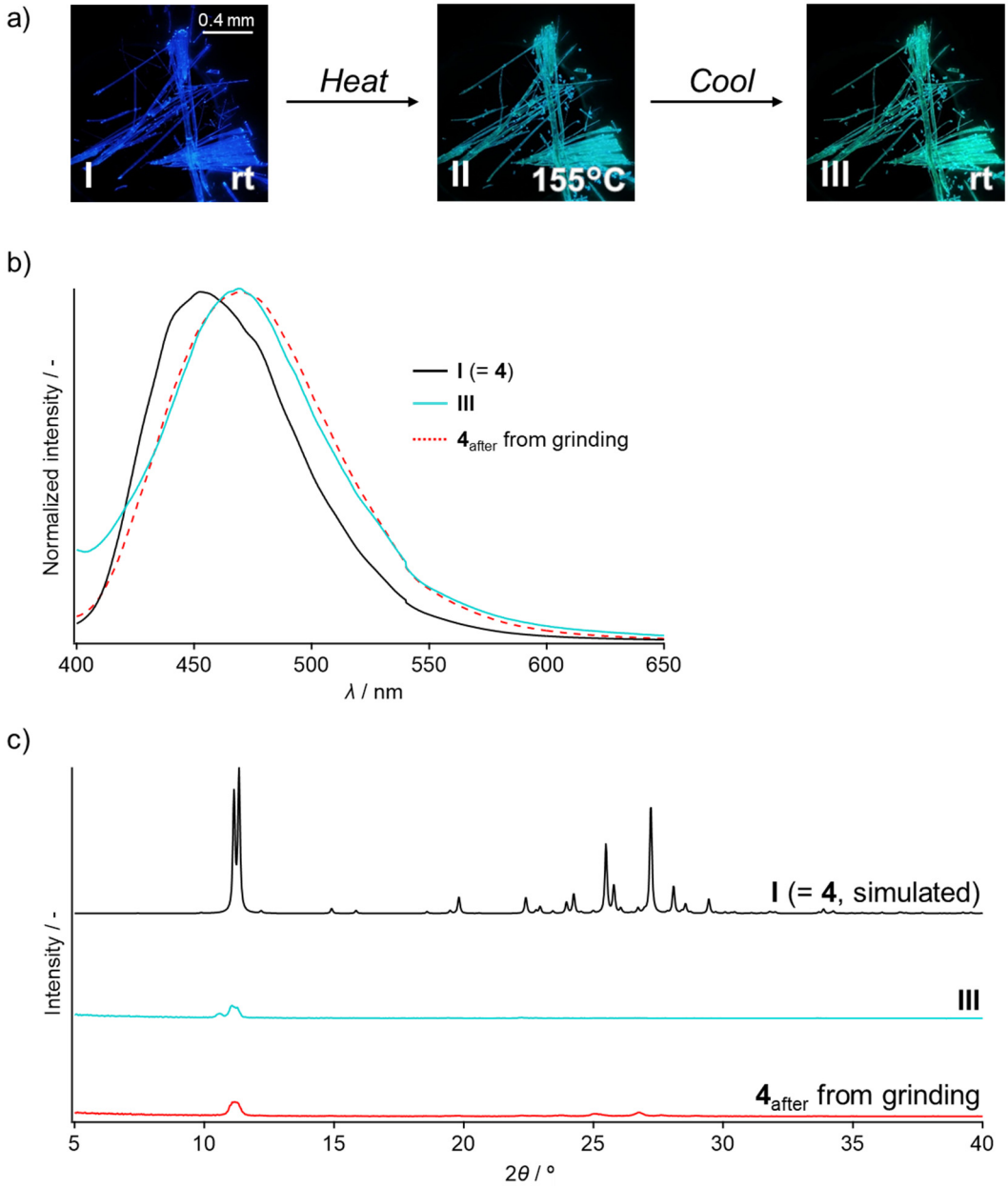


**Fig. S15** a) Photographs of **4** upon heating and subsequent cooling (under UV light). b) Emission spectra of **4** [the sample denoted as "**I**" in a), black line], the thermally treated sample [denoted as "**III**" in a), light blue line] and $\mathbf{4}_{after}$ obtained by grinding (reference, red dotted line). Excitation at 365 nm. c) A simulated powder pattern of **4** [the sample denoted as "**I**" in a), black line] and PXRD patterns of the thermally treated sample [denoted as "**III**" in a), light blue line] and $\mathbf{4}_{after}$ obtained by mechanical stimulation (red line).

## 8. Sublimation of 1 and 4

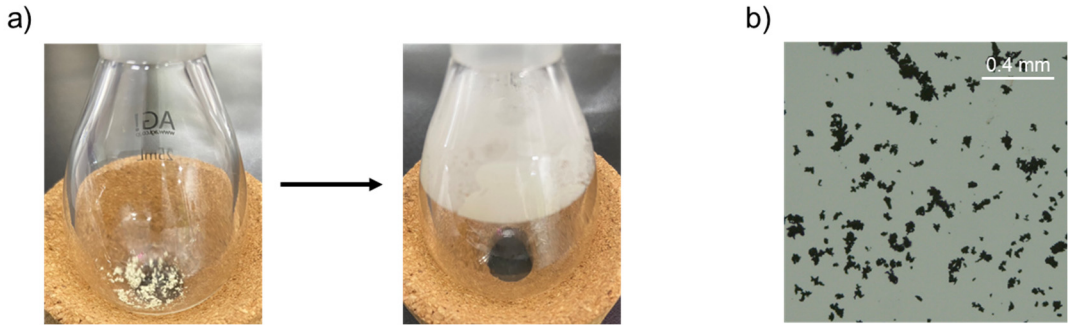


**Fig. S16** a) Photographs of the solid samples of **1** before and after the sublimation experiment. b) Photographs of the sublimated solid of **1** derived from the upper part of the glassware.

Note: Under 2.5 mbar, the flask containing the solid samples of **1** was gradually heated. At 40°C, the sublimation was started. Further increase of the temperature resulted in the sublimation of all the samples of **1** at 100°C. The purity of the sublimated solid was confirmed by the $^{1}$H NMR study after dissolution in $CDCl_3$ as shown in Fig. S17. The crystallinity of the sublimated sample is implied by the clear birefringence under crossed Nicols observation (data not shown).

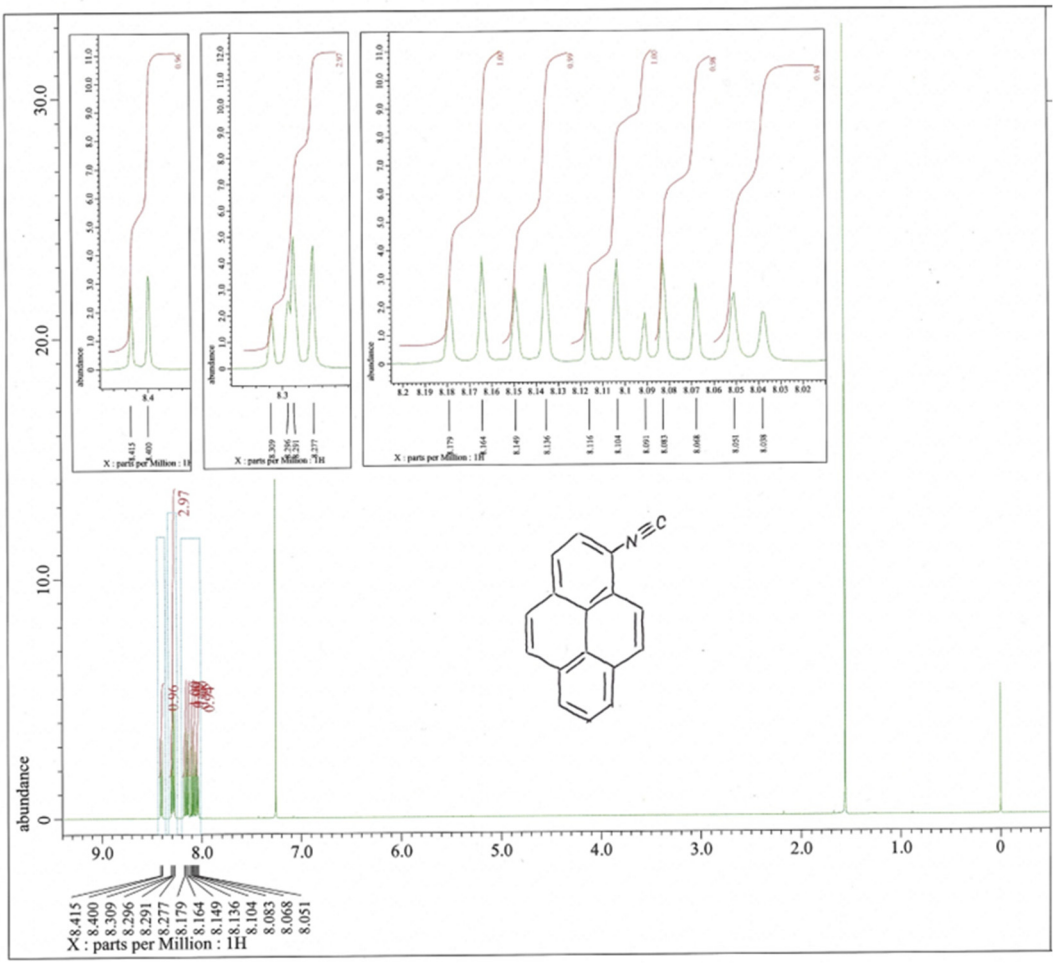


**Figure S17** NMR spectrum of the sublimated solid of **1** in $CDCl_3$.

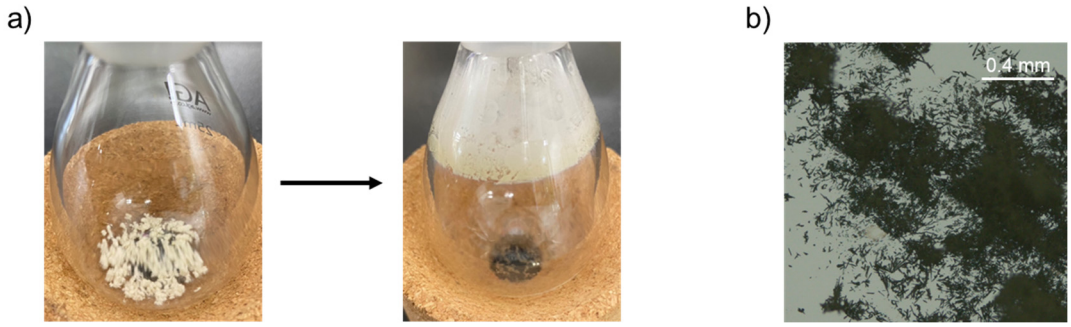


**Fig. S18** a) Photographs of the solid samples of **4** before and after the sublimation experiment. b) Photographs of the sublimated solid of **4** derived from the upper part of the glassware.

Note: Under 2.5 mbar, the flask containing the solid samples of **4** was gradually heated. At 50°C, the sublimation was started. Further increase of the temperature resulted in the sublimation of almost all the samples of **4** at 120°C. The purity of the sublimated solid was confirmed by the $^{1}$H NMR study after dissolution in $CDCl_3$ as shown in Fig. S19. The crystallinity of the sublimated sample is implied by the clear birefringence under crossed Nicols observation (data not shown).

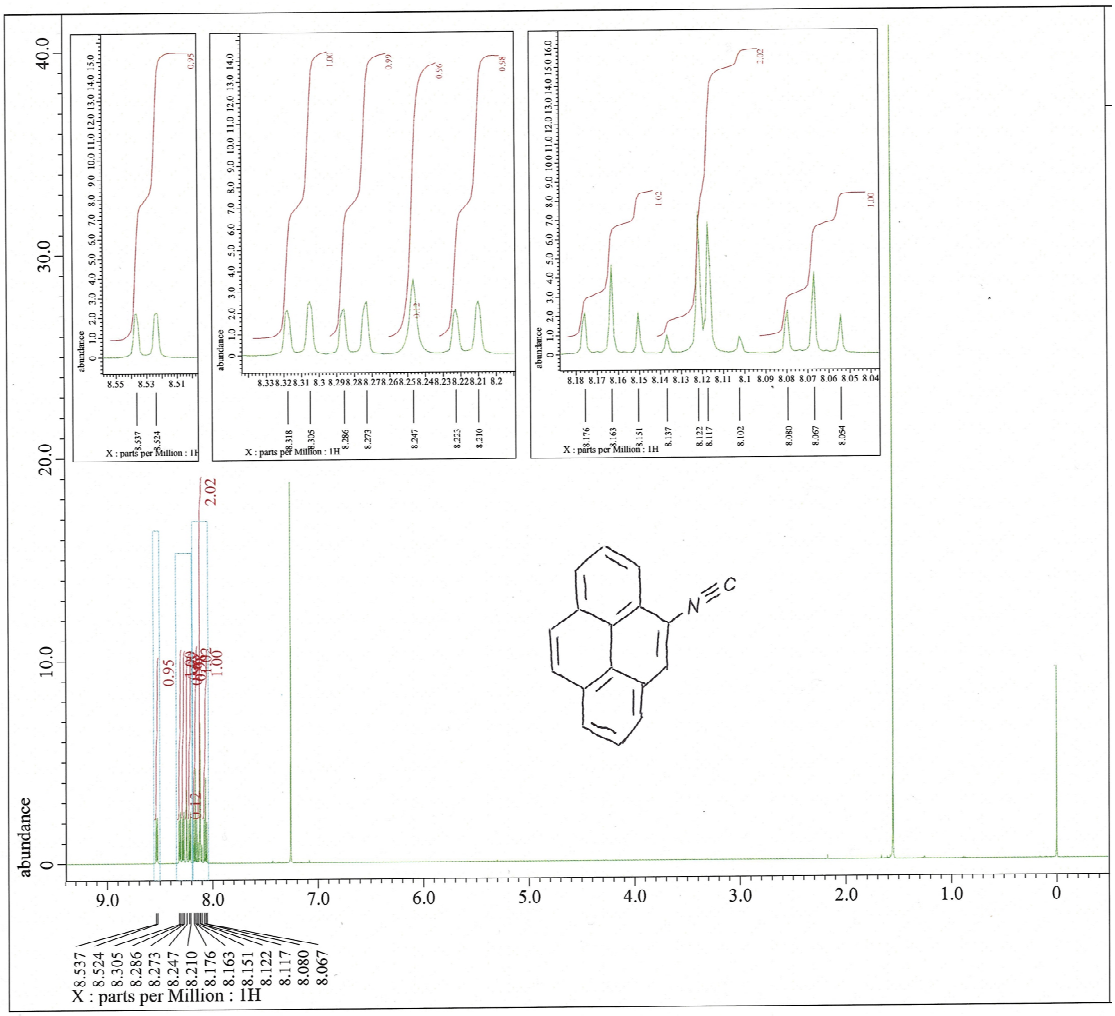


**Figure S19** NMR spectrum of the sublimated solid of **4** in $CDCl_3$.

## 9. References


[S1] Sheldrick, G. M. SHTLXT - Integrated space-group and crystal-structure determination. *Acta Cryst.* **2015**, *A71*, 3–8.

[S2] Sheldrick, G. M. Crystal structure refinement with SHELXL. *Acta Cryst.* **2015**, C*71,* 3–8.

[S3] Dolomanov, O. V.; Bourhis, L. J.; Gildea, R. J.; Howard, J. A. K.; Puschmann, H. OLEX2: a complete structure solution, refinement and analysis program. *J. Appl. Crystallogr.* **2009**, *42,* 339–341.

[S4] Macrae, C. F.; Sovago, I.; Cottrell, S. J.; Galek, P. T. A.; McCabe, P.; Pidcock, E.; Platings, M.; Shields, G. P.; Stevens, J. S.; Towler, M.; Wood, P. A. Mercury 4.0: from visualization to analysis, design and prediction. *J. Appl. Crystallogr.* **2020***, 53*, 226–235.

[S5] For the synthesis of 4-aminopyrene, see: J. A. Mikroyannidis, M. M. Stylianakis, M. S. Roy, P. Suresh, G. D. Sharma, *J. Power Sources*, **2009**, *194*, 1171–1179.

[S6] For the synthesis of **1**, see: X.-Y. Wang, J. Zhang, J. Yin, S. H. Liu, *Chem. Asian. J.*, **2019**, *14*, 2903–2910.

[S7] For the single crystal structure of **1**, see: E. S. Cueny, H. C. Johnson, B. J. Anding, C. R. Landis, *J. Am. Chem. Soc.*, **2017**, *139*, 11903–11912.

[S8] Gaussian 09, Revision C.01, M. J. Frisch, G. W. Trucks, H. B. Schlegel, G. E. Scuseria, M. A. Robb, J. R. Cheeseman, G. Scalmani, V. Barone, B. Mennucci, G. A. Petersson, H. Nakatsuji, M. Caricato, X. Li, H. P. Hratchian, A. F. Izmaylov, J. Bloino, G. Zheng, J. L. Sonnenberg, M. Hada, M. Ehara, K. Toyota, R. Fukuda, J. Hasegawa, M. Ishida, T. Nakajima, Y. Honda, O. Kitao, H. Nakai, T. Vreven, J. A. Montgomery, Jr., J. E. Peralta, F. Ogliaro, M. Bearpark, J. J. Heyd, E. Brothers, K. N. Kudin, V. N. Staroverov, R. Kobayashi, J. Normand, K. Raghavachari, A. Rendell, J. C. Burant, S. S. Iyengar, J. Tomasi, M. Cossi, N. Rega, J. M. Millam, M. Klene, J. E. Knox, J. B. Cross, V. Bakken, C. Adamo, J. Jaramillo, R. Gomperts, R. E. Stratmann, O. Yazyev, A. J. Austin, R. Cammi, C. Pomelli, J. W. Ochterski, R. L. Martin, K. Morokuma, V. G. Zakrzewski, G. A. Voth, P. Salvador, J. J. Dannenberg, S. Dapprich, A. D. Daniels, Ö. Farkas, J. B. Foresman, J. V. Ortiz, J. Cioslowski, and D. J. Fox, Gaussian, Inc., Wallingford CT, 2009.

[S9] F. Würthner, *Acc. Chem. Res.*, **2016**, *49*, 868–876.

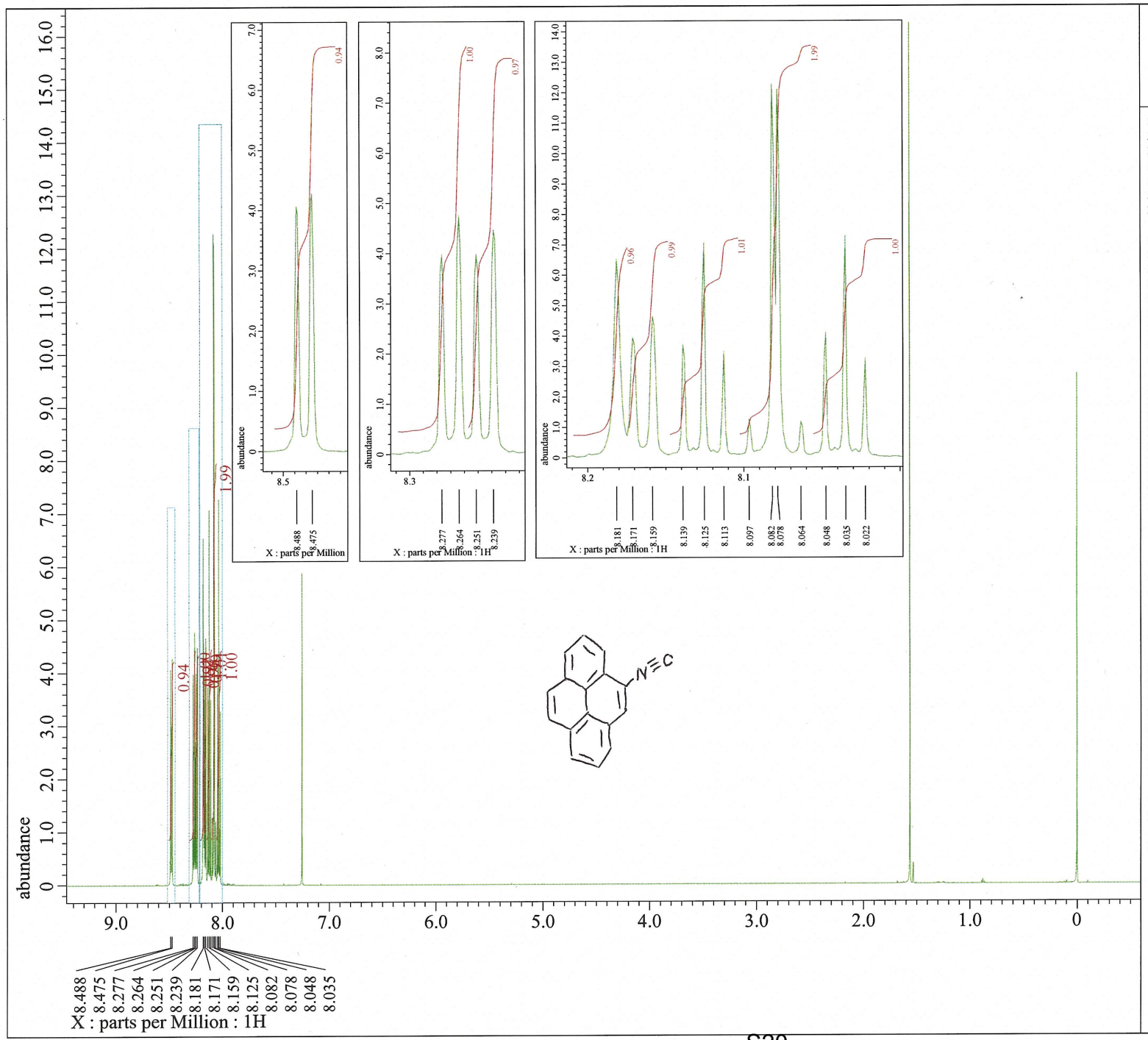


JEOL

```
Filename            = STS230912HTR-4-IP-2.jdf
Author              = delta
Experiment          = single_pulse.ex2
Sample_Id           = S#467284
Solvent             = CHLOROFORM-D
Actual_Start_Time   = 12-SEP-2023 21:28:22
Revision_Time       = 29-NOV-2023 11:24:13

Comment             = single_pulse
Data_Format         = 1D COMPLEX
Dim_Size            = 13107
X_Domain            = 1H
Dim_Title           = 1H
Dim_Units           = [ppm]
Dimensions          = X
Site                = ECA 600
Spectrometer        = DELTA2_NMR

Field_Strength      = 14.09636928[T] (600[MHz])
X_Acq_Duration      = 1.4548992[s]
X_Domain            = 1H
X_Freq              = 600.1723046[MHz]
X_Offset            = 5[ppm]
X_Points            = 16384
X_Prescans          = 1
X_Resolution        = 0.68733284[Hz]
X_Sweep             = 11.26126126[kHz]
Irr_Domain          = 1H
Irr_Freq            = 600.1723046[MHz]
Irr_Offset          = 5[ppm]
Tri_Domain          = 1H
Tri_Freq            = 600.1723046[MHz]
Tri_Offset          = 5[ppm]
Clipped             = FALSE
Scans               = 8
Total_Scans         = 8

Relaxation_Delay    = 5[s]
Recvr_Gain          = 46
Temp_Get            = 23.1[dC]
X_90_Width          = 8.3[us]
X_Acq_Time          = 1.4548992[s]
X_Angle             = 45[deg]
X_Atn               = 5[dB]
X_Pulse             = 4.15[us]
Irr_Mode            = Off
Tri_Mode            = Off
Dante_Presat        = FALSE
Initial_Wait        = 1[s]
Repetition_Time     = 6.4548992[s]
```

$^1H$

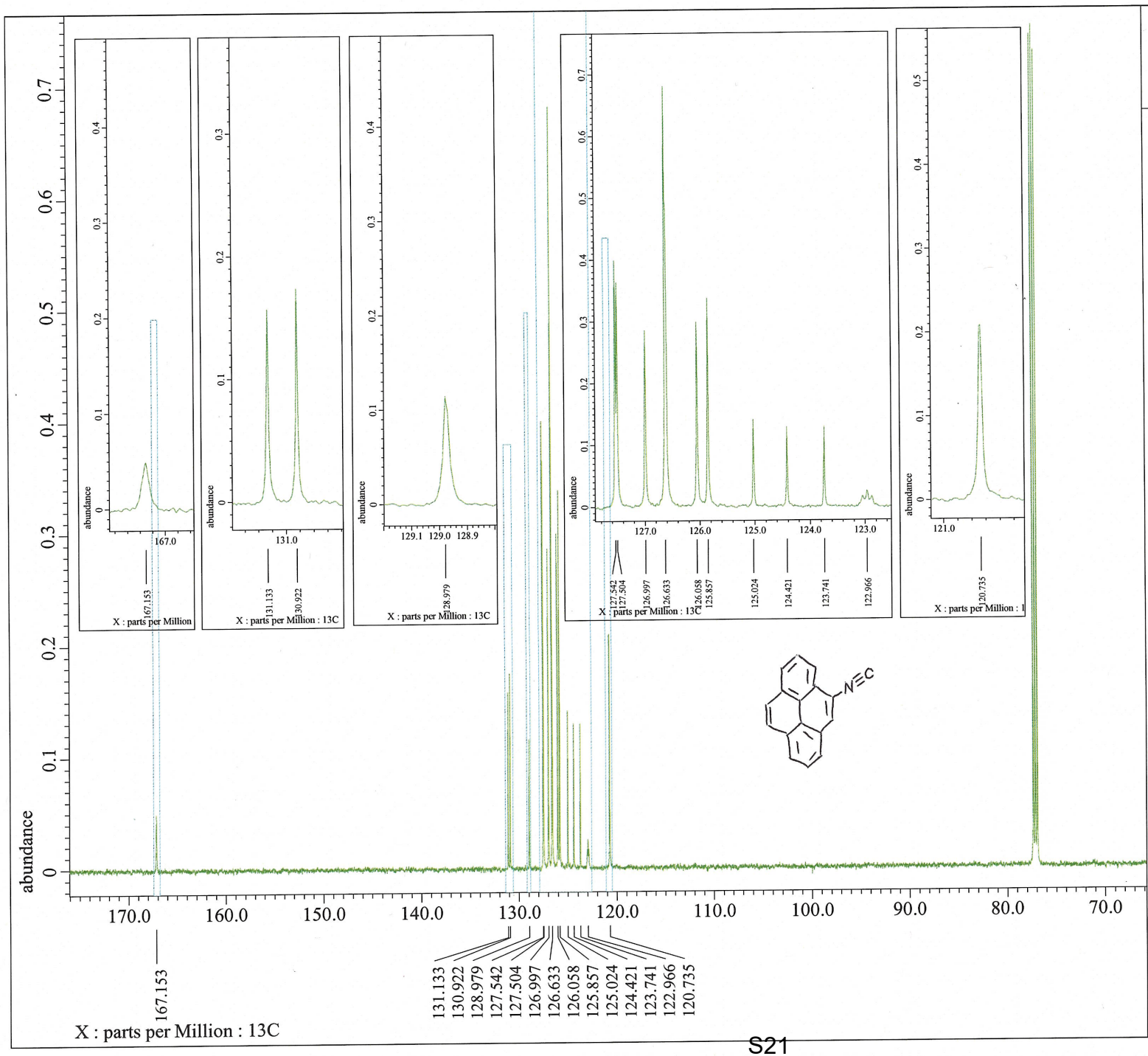


JEOL

| | |
|---|---|
| Filename | = STS230914HTR-4-IP-13C-2.j |
| Author | = delta |
| Experiment | = single_pulse_dec |
| Sample_Id | = S#336639 |
| Solvent | = CHLOROFORM-D |
| Actual_Start_Time | = 14-SEP-2023 17:50:36 |
| Revision_Time | = 29-NOV-2023 11:31:16 |
| Comment | = single pulse decoupled ga |
| Data_Format | = 1D COMPLEX |
| Dim_Size | = 26214 |
| X_Domain | = 13C |
| Dim_Title | = 13C |
| Dim_Units | = [ppm] |
| Dimensions | = X |
| Site | = ECA 600 |
| Spectrometer | = DELTA2_NMR |
| Field_Strength | = 14.09636928[T] (600[MHz]) |
| X_Acq_Duration | = 0.69206016[s] |
| X_Domain | = 13C |
| X_Freq | = 150.91343039[MHz] |
| X_Offset | = 100[ppm] |
| X_Points | = 32768 |
| X_Prescans | = 4 |
| X_Resolution | = 1.44496109[Hz] |
| X_Sweep | = 47.34848485[kHz] |
| Irr_Domain | = 1H |
| Irr_Freq | = 600.1723046[MHz] |
| Irr_Offset | = 5[ppm] |
| Clipped | = FALSE |
| Scans | = 1024 |
| Total_Scans | = 1024 |
| Relaxation_Delay | = 2[s] |
| Recvr_Gain | = 50 |
| Temp_Get | = 23.2[dC] |
| X_90_Width | = 11.2[us] |
| X_Acq_Time | = 0.69206016[s] |
| X_Angle | = 30[deg] |
| X_Atn | = 4[dB] |
| X_Pulse | = 3.73333333[us] |
| Irr_Atn_Dec | = 24.085[dB] |
| Irr_Atn_Noe | = 24.085[dB] |
| Irr_Noise | = WALTZ |
| Decoupling | = TRUE |
| Initial_Wait | = 1[s] |
| Noe | = TRUE |
| Noe_Time | = 2[s] |
| Repetition_Time | = 2.69206016[s] |

$^{13}C$

C:\Users\...\231116_seki_01_APCI 2023/11/16 18:06:12

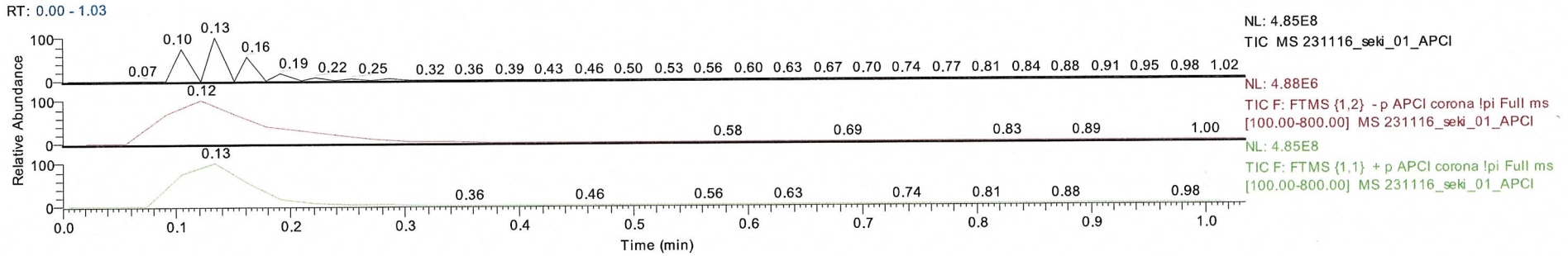


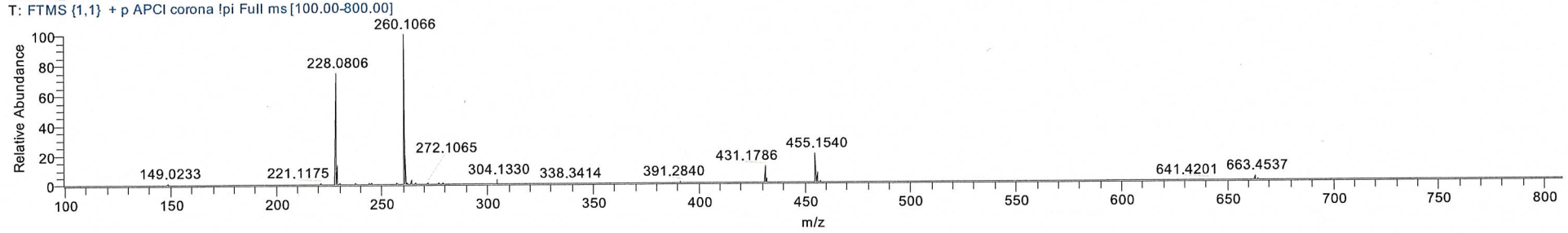


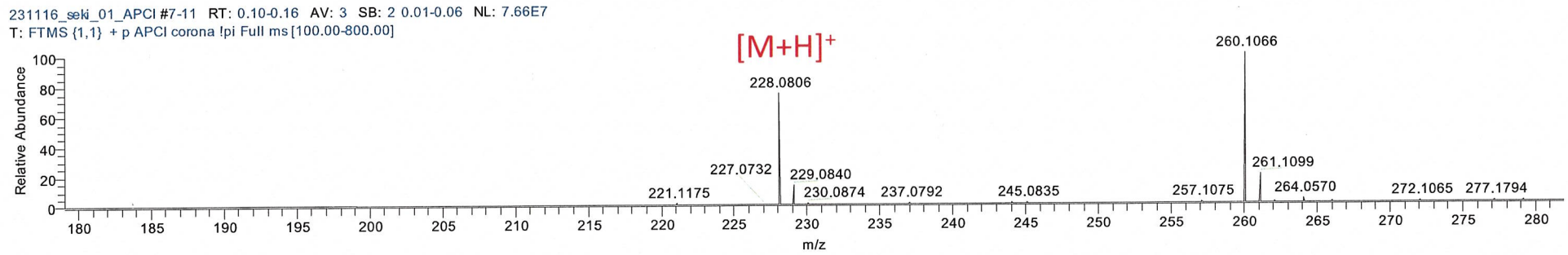


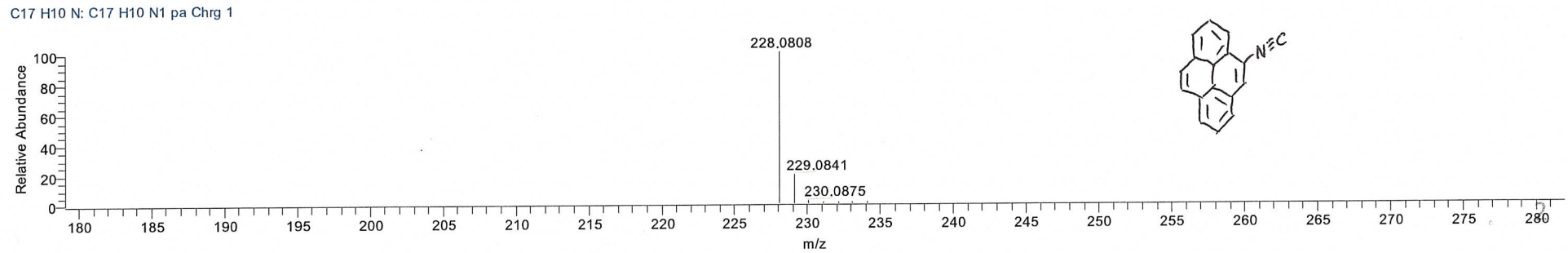

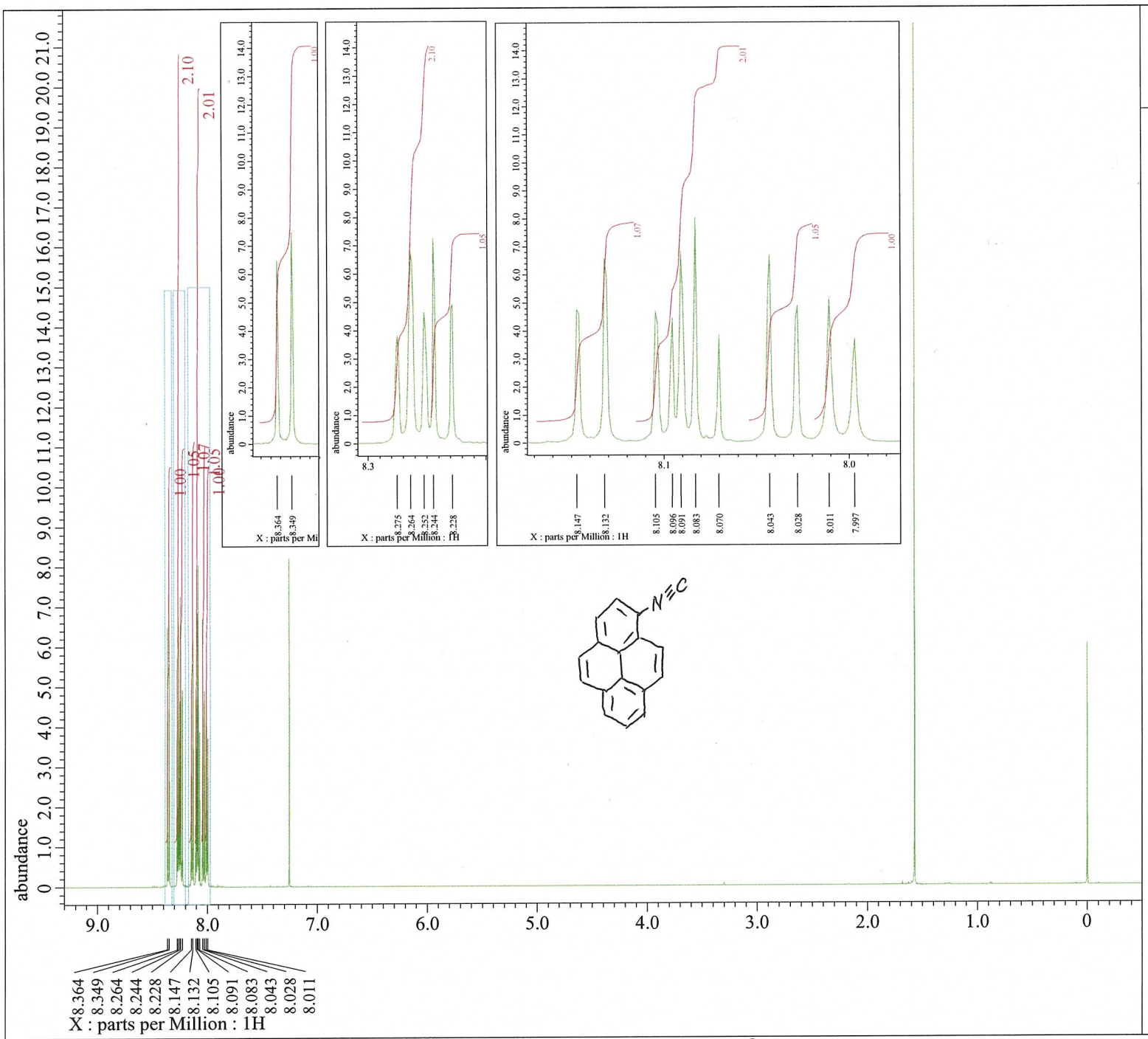


JEOL

| | |
|---|---|
| Filename | = STS230620HTR-358-2.jdf |
| Author | = delta |
| Experiment | = single_pulse.ex2 |
| Sample_Id | = S#592455 |
| Solvent | = CHLOROFORM-D |
| Actual_Start_Time | = 21-JUN-2023 00:56:51 |
| Revision_Time | = 15-FEB-2024 09:18:40 |
| Comment | = single_pulse |
| Data_Format | = 1D COMPLEX |
| Dim_Size | = 13107 |
| X_Domain | = 1H |
| Dim_Title | = 1H |
| Dim_Units | = [ppm] |
| Dimensions | = X |
| Site | = ECA 600 |
| Spectrometer | = DELTA2_NMR |
| Field_Strength | = 14.09636928[T] (600[MHz]) |
| X_Acq_Duration | = 1.4548992[s] |
| X_Domain | = 1H |
| X_Freq | = 600.1723046[MHz] |
| X_Offset | = 5[ppm] |
| X_Points | = 16384 |
| X_Prescans | = 1 |
| X_Resolution | = 0.68733284[Hz] |
| X_Sweep | = 11.26126126[kHz] |
| Irr_Domain | = 1H |
| Irr_Freq | = 600.1723046[MHz] |
| Irr_Offset | = 5[ppm] |
| Tri_Domain | = 1H |
| Tri_Freq | = 600.1723046[MHz] |
| Tri_Offset | = 5[ppm] |
| Clipped | = FALSE |
| Scans | = 8 |
| Total_Scans | = 8 |
| Relaxation_Delay | = 5[s] |
| Recvr_Gain | = 46 |
| Temp_Get | = 22.6[dC] |
| X_90_Width | = 8.3[us] |
| X_Acq_Time | = 1.4548992[s] |
| X_Angle | = 45[deg] |
| X_Atn | = 5[dB] |
| X_Pulse | = 4.15[us] |
| Irr_Mode | = Off |
| Tri_Mode | = Off |
| Dante_Presat | = FALSE |
| Initial_Wait | = 1[s] |
| Repetition_Time | = 6.4548992[s] |

1H